ISSN 1948-9358 (online)

World Journal of *Diabetes*

World J Diabetes 2023 July 15; 14(7): 939-1145

Published by Baishideng Publishing Group Inc

World Journal of Diabetes

Contents

Monthly Volume 14 Number 7 July 15, 2023

OPINION REVIEW

939 Access to novel anti-diabetic agents in resource limited settings: A brief commentary

Naidoo P, Naidoo K, Karamchand S, Leisegang RF

REVIEW

942 Detection, management, and prevention of diabetes-related foot disease in the Australian context

McNeil S, Waller K, Poy Lorenzo YS, Mateevici OC, Telianidis S, Qi S, Churilov I, MacIsaac RJ, Galligan A

958 Novel insights regarding the role of noncoding RNAs in diabetes

Macvanin MT, Gluvic Z, Bajic V, Isenovic ER

977 Implications of receptor for advanced glycation end products for progression from obesity to diabetes and from diabetes to cancer

Garza-Campos A, Prieto-Correa JR, Domínguez-Rosales JA, Hernández-Nazará ZH

995 Advanced glycation end product signaling and metabolic complications: Dietary approach

Khan MI, Ashfaq F, Alsayegh AA, Hamouda A, Khatoon F, Altamimi TN, Alhodieb FS, Beg MMA

1013 Tight junction disruption and the pathogenesis of the chronic complications of diabetes mellitus: A narrative review

Robles-Osorio ML, Sabath E

MINIREVIEWS

1027 Klotho: A new therapeutic target in diabetic retinopathy?

Puddu A, Maggi DC

1037 Type 2 diabetes and thyroid cancer: Synergized risk with rising air pollution

Kruger EM, Shehata SA, Toraih EA, Abdelghany AA, Fawzy MS

1049 Liver or kidney: Who has the oar in the gluconeogenesis boat and when?

Sahoo B, Srivastava M, Katiyar A, Ecelbarger C, Tiwari S

ORIGINAL ARTICLE

Basic Study

1057 Network-pharmacology-based research on protective effects and underlying mechanism of Shuxin decoction against myocardial ischemia/reperfusion injury with diabetes

Yang L, Jian Y, Zhang ZY, Qi BW, Li YB, Long P, Yang Y, Wang X, Huang S, Huang J, Zhou LF, Ma J, Jiang CQ, Hu YH, Xiao WJ

World Journal of Diabetes

Monthly Volume 14 Number 7 July 15, 2023

Contents

1077 Analysis of N6-methyladenosine-modified mRNAs in diabetic cataract

Cai L, Han XY, Li D, Ma DM, Shi YM, Lu Y, Yang J

Retrospective Cohort Study

1091 Long-term quality-of-care score for predicting the occurrence of acute myocardial infarction in patients with type 2 diabetes mellitus

Li PI, Guo HR

Retrospective Study

1103 Correlation between glycated hemoglobin A1c, urinary microalbumin, urinary creatinine, β2 microglobulin, retinol binding protein and diabetic retinopathy

Song JJ, Han XF, Chen JF, Liu KM

Observational Study

1112 Glucose metabolism profile recorded by flash glucose monitoring system in patients with hypopituitarism during prednisone replacement

Han MM, Zhang JX, Liu ZA, Xu LX, Bai T, Xiang CY, Zhang J, Lv DQ, Liu YF, Wei YH, Wu BF, Zhang Y, Liu YF

1126 Association between cardiorespiratory fitness level and insulin resistance in adolescents with various obesity categories

La Grasta Sabolic L, Pozgaj Sepec M, Valent Moric B, Cigrovski Berkovic M

CASE REPORT

1137 Maturity-onset diabetes of the young type 9 or latent autoimmune diabetes in adults: A case report and review of literature

Zhou GH, Tao M, Wang Q, Chen XY, Liu J, Zhang LL

World Journal of Diabetes

Monthly Volume 14 Number 7 July 15, 2023

Contents

ABOUT COVER

Editorial Board Member of *World Journal of Diabetes*, Sonia Eiras, BSc, PhD, Senior Researcher, Traslational Cardiology, Health Research Institute, University Hospital of Santiago de Compostela, Santiago de Compostela 15706, Spain. sonia.eiras.penas@sergas.es

AIMS AND SCOPE

The primary aim of *World Journal of Diabetes* (*WJD*, *World J Diabetes*) is to provide scholars and readers from various fields of diabetes with a platform to publish high-quality basic and clinical research articles and communicate their research findings online.

WJD mainly publishes articles reporting research results and findings obtained in the field of diabetes and covering a wide range of topics including risk factors for diabetes, diabetes complications, experimental diabetes mellitus, type 1 diabetes mellitus, type 2 diabetes mellitus, gestational diabetes, diabetic angiopathies, diabetic cardiomyopathies, diabetic coma, diabetic ketoacidosis, diabetic nephropathies, diabetic neuropathies, Donohue syndrome, fetal macrosomia, and prediabetic state.

INDEXING/ABSTRACTING

The *WJD* is now abstracted and indexed in Science Citation Index Expanded (SCIE, also known as SciSearch®), Current Contents/Clinical Medicine, Journal Citation Reports/Science Edition, PubMed, PubMed Central, Reference Citation Analysis, China National Knowledge Infrastructure, China Science and Technology Journal Database, and Superstar Journals Database. The 2023 Edition of Journal Citation Reports® cites the 2022 impact factor (IF) for *WJD* as 4.2; IF without journal self cites: 4.1; 5-year IF: 4.5; Journal Citation Indicator: 0.69; Ranking: 51 among 145 journals in endocrinology and metabolism; and Quartile category: Q2.

RESPONSIBLE EDITORS FOR THIS ISSUE

NAME OF JOURNAL
World Journal of Diabetes

ISSN
ISSN 1948-9358 (online)

LAUNCH DATE
June 15, 2010

FREQUENCY
Monthly

PUBLICATION DATE
July 15, 2023

World Journal of Diabetes

Submit a Manuscript: https://www.f6publishing.com

World J Diabetes 2023 July 15; 14(7): 1077-1090

DOI: 10.4239/wjd.v14.i7.1077

ISSN 1948-9358 (online)

ORIGINAL ARTICLE

Basic Study

Analysis of N6-methyladenosine-modified mRNAs in diabetic cataract

Lei Cai, Xiao-Yan Han, Dan Li, Dong-Mei Ma, Yu-Meng Shi, Yi Lu, Jin Yang

Specialty type: Ophthalmology

Provenance and peer review: Unsolicited article; Externally peer reviewed.

Peer-review model: Single blind

Peer-review report's scientific quality classification

Grade A (Excellent): 0
Grade B (Very good): B
Grade C (Good): C
Grade D (Fair): 0
Grade E (Poor): 0

P-Reviewer: Godfrey KM, United Kingdom; Sathish T, Canada

Received: March 6, 2023
Peer-review started: March 6, 2023
First decision: March 14, 2023
Revised: March 27, 2023
Accepted: April 27, 2023
Article in press: April 27, 2023
Published online: July 15, 2023

Lei Cai, Xiao-Yan Han, Dan Li, Dong-Mei Ma, Yu-Meng Shi, Yi Lu, Jin Yang, Department of Ophthalmology, Eye, Ear, Nose, and Throat Hospital of Fudan University, Shanghai 200031, China

Lei Cai, Xiao-Yan Han, Dan Li, Dong-Mei Ma, Yu-Meng Shi, Yi Lu, Jin Yang, Key Laboratory of Myopia, Ministry of Health, Shanghai 200031, China

Lei Cai, Xiao-Yan Han, Dan Li, Dong-Mei Ma, Yu-Meng Shi, Yi Lu, Jin Yang, Shanghai Key Laboratory of Visual Impairment and Restoration, Shanghai Key Laboratory of Visual Impairment and Restoration, Shanghai 200031, China

Lei Cai, Xiao-Yan Han, Dan Li, Dong-Mei Ma, Yu-Meng Shi, Yi Lu, Jin Yang, Visual Rehabilitation Professional Committee, Chinese Association of Rehabilitation Medicine, Shanghai 200031, China

Dan Li, State Key Laboratory of Molecular Engineering of Polymers, Fudan University, Shanghai 200031, China

Corresponding author: Jin Yang, MD, Chief Physician, Department of Ophthalmology, Eye, Ear, Nose, and Throat Hospital of Fudan University, No. 83 Fenyang Road, Shanghai 200031, China. jin_er76@hotmail.com

Abstract

BACKGROUND

Cataracts remain a prime reason for visual disturbance and blindness all over the world, despite the capacity for successful surgical replacement with artificial lenses. Diabetic cataract (DC), a metabolic complication, usually occurs at an earlier age and progresses faster than age-related cataracts. Evidence has linked N6-methyladenosine (m6A) to DC progression. However, there exists a lack of understanding regarding RNA m6A modifications and the role of m6A in DC pathogenesis.

AIM

To elucidate the role played by altered m6A and differentially expressed mRNAs (DEmRNAs) in DC.

METHODS

Anterior lens capsules were collected from the control subjects and patients with

DC. M6A epitranscriptomic microarray was performed to investigate the altered m6A modifications and determine the DEmRNAs. Through Gene Ontology and pathway enrichment (Kyoto Encyclopedia of Genes and Genomes) analyses, the potential role played by dysregulated m6A modification was predicted. Real-time polymerase chain reaction was further carried out to identify the dysregulated expression of RNA methyltransferases, demethylases, and readers.

RESULTS

Increased m6A abundance levels were found in the total mRNA of DC samples. Bioinformatics analysis predicted that ferroptosis pathways could be associated with m6A-modified mRNAs. The levels of five methylation-related genes-*RBM15*, *WTAP*, *ALKBH5*, *FTO*, and *YTHDF1*-were upregulated in DC samples. Upregulation of *RBM15* expression was verified in SRA01/04 cells with high-glucose medium and in samples from DC patients.

CONCLUSION

M6a mRNA modifications may be involved in DC progression *via* the ferroptosis pathway, rendering novel insights into therapeutic strategies for DC.

Key Words: N6-methyladenosine; Diabetic cataract; RNA; Ferroptosis; Epitranscriptomic microarray

Core Tip: Diabetic cataracts (DCs) are associated with elevated blood sugar levels and usually occur at an earlier age with more rapid progression than age-related cataracts. However, the specific molecular mechanisms underlying DC progression remain to be elucidated. As environmental factors are essential in the pathogenesis of diabetes mellitus, epigenetic changes may be particularly important. Recently, N6-methyladenosine (m6A) has been suggested to play a part in DC progression. The present study elucidated the m6A landscape in DC and simultaneously analyzed the methylation and expression of related mRNA. These analyses indicate that m6A mRNA modifications in lens epithelial cells might be involved in DC progression.

Citation: Cai L, Han XY, Li D, Ma DM, Shi YM, Lu Y, Yang J. Analysis of N6-methyladenosine-modified mRNAs in diabetic cataract. *World J Diabetes* 2023; 14(7): 1077-1090
URL: https://www.wjgnet.com/1948-9358/full/v14/i7/1077.htm
DOI: https://dx.doi.org/10.4239/wjd.v14.i7.1077

INTRODUCTION

Over the last several decades, the prevalence of diabetes mellitus (DM) in adults has increased globally. There were approximately 110 million DM cases in China in 2015, and the number is estimated to be 150 million by 2040, as indicated by the International Diabetes Federation[1]. DM, a systemic condition, affects various organs and thus can induce several complications, including cataracts[2]. Despite the increasing maturity of modern cataract surgery technology, cataracts remain a prime reason for vision loss and blindness globally[3,4]. Diabetic cataracts (DCs) usually develop at an earlier age and pro-gresses more rapidly than age-related cataracts do[5]. Evidence has linked DC to polyol pathway, nonenzymatic glycation, and oxidative stress (OS)[4]. Yet, the molecular mechanism underlying DC progression remains largely unknown.

As environmental factors play critical roles in the pathogenesis of DM, epigenetic changes may be particularly important[6]. N6-methyladenosine (m6A), one of the most prevalent epigenetic modifications in mammals[7], is increasingly shown to be crucial in several pathological processes (*e.g.*, tumorigenesis, angiogenesis, tissue degeneration, and inflammatory responses)[8,9]. A study on DC patho-genesis based on m6A-RNA immunoprecipitation (MeRIP)-sequencing reported that the level of the methyltransferase protein complex, methyltransferase-like 3 (METTL3), is upregulated in high glucose-induced human lens epithelial cells (LECs) and that METTL3 mediates a higher methylation level[10]. However, the RNA m6A modification landscape in DC and the role of m6A in DC pathogenesis are still largely undetermined.

Herein, we performed an m6A epitranscriptomic microarray analysis to identify differentially methylated mRNAs and determined their potential roles using bioinformatics analyses, rendering novel insights into the pathogenic mechanisms of DC as well as clues for future biological interventions.

MATERIALS AND METHODS

Participants and specimen collection

The anterior lens capsule (ALC) tissue of three DC patients had been living with diabetes for more than 5 years was collected, and the cataract severity was graded using the Lens Opacities Classification System III[11]. In addition, ALCs collected from age-matched transparent crystals of cadaveric eyes were used as normal controls (NC). Patients with other eye diseases, such as high myopia, trauma, uveitis, or glaucoma were excluded from the study. Patients' information is presented in Table 1. The workflow of sample collection and processing is shown in Figure 1. This study has obtained approval from the Ethics Committee of the Eye and ENT Hospital of Fudan University and written informed consent from all participants, and the principles of the Declaration of Helsinki were strictly follows throughout the research period. This study was registered with ClinicalTrials.gov, number NCT05682001.

Cell culture

The human LEC line SRA01/04, obtained from Genechem, was immersed in Dulbecco's modified Eagle's medium (Thermo Fisher Scientific, United States) where 5.5 mmol/L glucose, 10% fetal bovine serum (Invitrogen, Carlsbad, CA, United States), 100 IU/mL penicillin (Thermo Fisher Scientific), and 100 mg/mL streptomycin (Thermo Fisher Scientific) were added, for cultivation in a 5% CO_2 humidified atmosphere with the temperature maintained at 37 °C. Confluent cells (75%-80%) were then randomly grouped as a normal- (NG group; 5.5 mmol/L glucose-supplemented medium) and a high-glucose group (HG group; 25.0 mmol/L glucose-supplemented medium), and cultured for 24 h for subsequent examinations.

Total RNA extraction and m6A immunoprecipitation

Using TRIzol (Invitrogen) and following kit recommendations, total RNA was isolated from the LECs of the included DC patients and controls, as well as SRA01/04 cells, followed by RNA quantification and purity evaluation with a NanoDrop ND-1000 spectrophotometer purchased from Thermo Fisher Scientific. This was followed by immunoprecipitation (IP) of the extracted total RNA from the NC (n = 3) and DC samples (n = 3) with an anti-m6A antibody by referring to the manufacturer's recommendations. In brief, we placed 2 μg total RNA and m6A spike-in control mixture into a 300 μL IP buffer supplemented with 2 μg anti-m6A rabbit polyclonal antibody (Synaptic Systems, Goettingen, Germany), and let the reaction mixture rotate head-over-tail for 2 h at 4 °C. A DynabeadsTM M-280 sheep anti-rabbit immunoglobulin G (IgG) suspension (20 μL) was blocked with freshly prepared 0.5% bovine serum albumin at 4 °C for 2 h, followed by three rinses with IP buffer (300 μL) and resuspension in the total RNA-antibody mixture prepared. The RNA was then allowed to bind to the m6A-antibody beads for 2 h at 4 °C *via* head-over-tail rotation. After washing the beads thrice with 500 μL 1 × IP buffer and twice with 500 μL wash buffer, and incubation with 200 μL elution buffer (50 °C, 1 h), the enriched RNA was eluted and extracted using acid phenol-chloroform for ethanol precipitation.

Two-color RNA labeling and hybridization

The immunoprecipitated m6A-enriched RNAs were eluted from the magnetic beads as "IP", while the unmodified RNAs were collected from the supernatant as "Sup", which were then labeled with Cy5 and Cy3 (cRNAs), respectively, using an Arraystar Super RNA Labeling Kit (Arraystar, AL-SE-005). Purification of the synthesized cRNAs employed a RNeasy Mini Kit (QIAGEN, 74105), and the determination of concentrations and specific activities used the NanoDrop ND-1000. Following Arraystar's standard protocol, microarray hybridization was performed. We combined and hybridized Cy3 and Cy5 Labeled cRNAs to an Arraystar Human mRNA Epitranscriptomic Microarray (4 × 44 K, Arraystar, China), after which the slices were washed for array scanning using an Agilent Scanner G2505C (Agilent, Beijing, China).

Data analysis

Analyses of the acquired array images were carried out using Agilent's Feature Extraction software *v*11.0.1.1. Cy5-labeled IP and Cy3-labeled Sup raw intensities were normalized to the mean of log_2-scaled spike-in RNA intensities. The m6A methylation level was counted as a percentage of modified RNA (% modified) from total RNA, based on IP and Sup normalized intensities. The m6A quantity of each transcript was calculated according to normalized IP (Cy5-labeled) intensities. RNA expression was determined from the total IP and Sup normalized RNA intensities.

Gene ontology and pathway analysis

The online gene ontology (GO) (URL: http://www.geneontology.org) and Kyoto Encyclopedia of Genes and Genomes (KEGG) databases (URL: http://www.genome.jp/kegg) were utilized for determining the enriched GO terms and pathways in the mRNAs with significantly different m6A expression levels.

MeRIP coupled with real-time quantitative polymerase chain reaction

To validate microarray data quality, MeRIP-quantitative polymerase chain reaction (qPCR) was performed on four randomly selected mRNAs. In brief, the IP RNAs from ALC tissues of patients with DC and NCs were analyzed for microarray data validation, with primers used presented in Supplementary Table 1.

Reverse transcription-qPCR

Reverse transcription of total RNA to cDNA was performed as per the instruction of the PrimeScript RT Reagent Kit (Takara, Dalian, Liaoning province, China). Reverse transcription-qPCR (qRT-PCR) primers, designed with the use of

Table 1 Features of diabetic cataract patients included in microarray analysis

No.	Gender	Age (yr)	AL (mm)	Lens opacity grading	Duration of DM (year)	FBG (mmol/L)	HbA1c (%)
1	Male	64	22.09	C4N3P3	10	7.89	7.50
2	Female	68	21.77	C3N4P4	7	8.30	7.80
3	Female	63	23.43	C4N4P5	7	8.30	7.90

AL: Axial length; FBG: Fasting blooding glucose; HbA1c: Hemoglobin; DM: Diabetes mellitus.

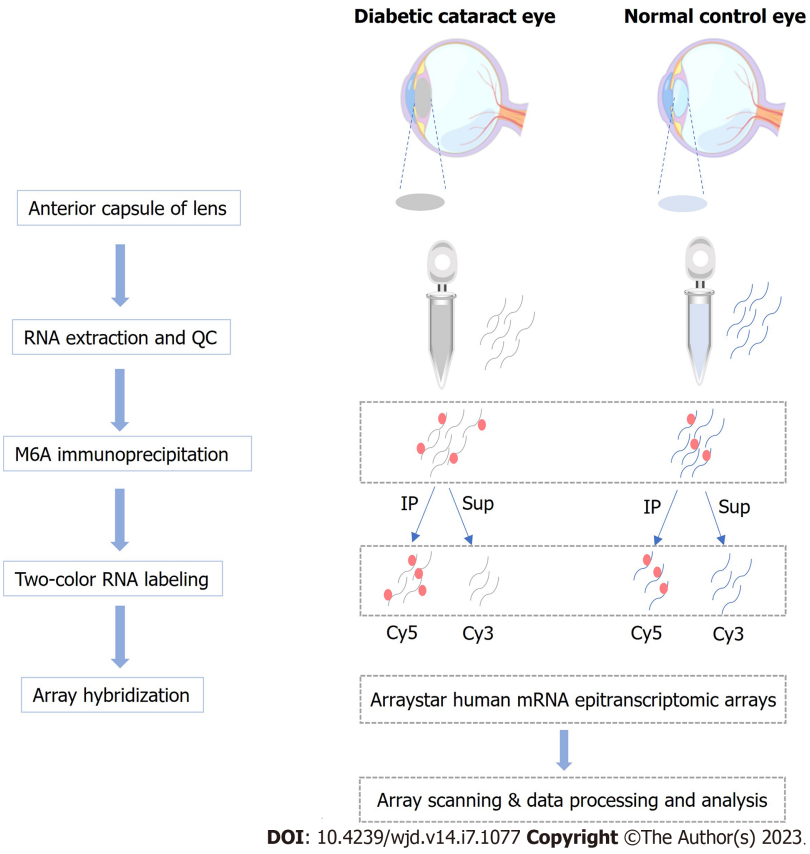

DOI: 10.4239/wjd.v14.i7.1077

Figure 1 Workflow of the experimental design. m6A: N6-methyladenosine; QC: Quality control; IP: Immunoprecipitation.

Primer 5.0, were blasted for specificity in NCBI (Supplementary Table 1). An Applied Biosystems ViiA 7 Real-Time thermal cycler (Thermo Fisher Scientific) and SYBR Green PCR Master Mix (Arraystar) were then utilized to perform the qRT-PCR. The expression of target mRNAs were normalized against Actin, and fold changes were determined by the comparative CT ($2^{-\Delta\Delta CT}$) method.

Statistical analysis

The significance threshold was $P < 0.05$ in this study. For the microarray analysis, statistical significance in methylation levels between DC cases and NCs was identified using an unpaired two-sided t-test. For GO and KEGG analyses, GO terms and KEGG pathway identifiers with significant differences were identified using the Fisher's exact test p-value and -log10(p) transformed as the enrichment score. While the relative genes' expression in MeRIP-qPCR and qRT-PCR was worked out by $2^{-\Delta\Delta CT}$.

RESULTS

Epitranscriptomic microarray analysis reveals the differential m6A modification of mRNAs in DC samples

Microarray analyses of the mRNAs extracted from the lens anterior capsule tissues of the DC and NC samples showed differential m6A-methylated mRNAs, as identified by the "m6A-mRNA quantity and m6A-mRNA methylation level". The results have been presented as heatmaps (Figure 2A and C) and volcano plots (Figure 2B and D). According to the

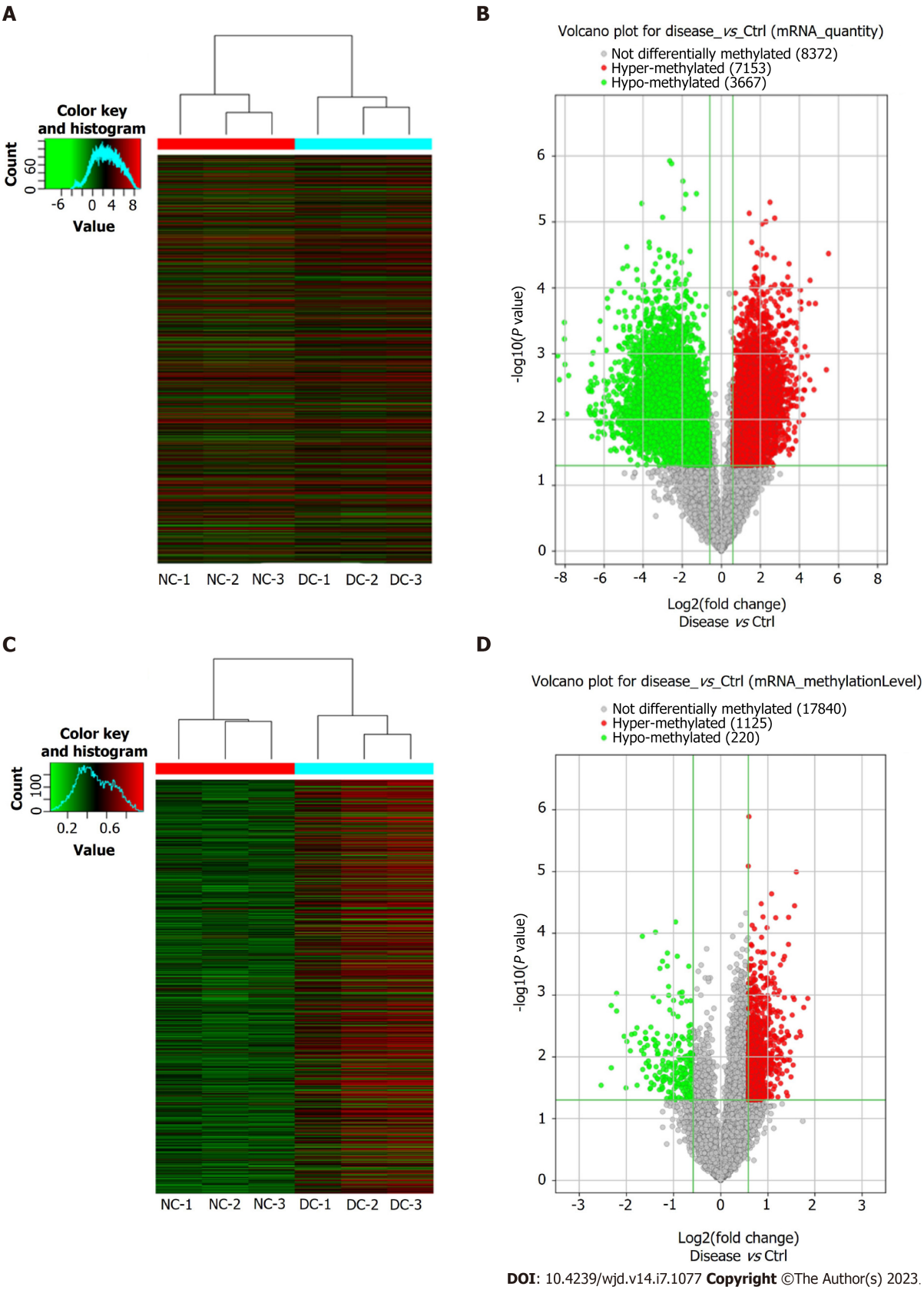

DOI: 10.4239/wjd.v14.i7.1077

Figure 2 Microarray data analysis showing expression profile of methylated mRNAs. A: Visualization of differential N6-methyladenosine (m6A) quantity profiles of mRNAs between the diabetic cataract (DC) and normal control (NC) groups through heat map and hierarchical clustering, where red and green colors indicate up- and down-regulated mRNAs, respectively; B: Volcano plot showing significant dysregulation of 10820 (7153 upregulated and 3667 downregulated) mRNAs in DC cases compared to NCs; C: Visualization of differential m6A mRNA methylation level profiles between DC cases and NCs through heat map and hierarchical clustering, where red and green colors indicate up- and down-regulated mRNAs, respectively; D: Volcano plot showing significant dysregulation of 1345 (1125 upregulated and 220 downregulated) methylated mRNAs in DC cases versus NCs.

m6A quantity results, there were 7153 hypermethylated mRNAs and 3667 hypomethylated mRNAs. As per the m6A methylation level results, 1125 mRNAs had higher m6A methylation levels, whereas 220 mRNAs had lower levels. See Table 2 for the top 20 mRNAs with the most significant hyper- and hypomethylation levels between DCs and NCs.

GO and KEGG pathway analyses reveal the biological function of differentially methylated mRNAs in DC

The enriched GO annotations can be fall into biological process (BP), cellular component (CC), or molecular function (MF). For hypermethylated mRNAs, 580 BPs, 110 CCs, and 100 MFs were enriched. The quantity of differentially methylated mRNAs related to the listed GO ID was recorded; of them, the top 10 most significantly enriched terms are presented as pie charts (Figure 3A-C, G). In addition, the top four terms with the highest enrichment score are shown in Figure 3G. For the hypomethylated mRNAs, 288 BPs, 47 CCs, and 67 MFs were enriched. See Figures 3D-F and H for the top 10 most significantly enriched terms and the top 4 terms with the highest enrichment scores.

Based on KEGG pathway analysis, the mRNAs differentially methylated by m6A participated in 27 pathways (Figure 4A and B). Most of the hypermethylated mRNAs were primarily enriched in "ferroptosis", "PPAR axis", and "alpha-linolenic acid metabolism". The ferroptosis pathway map is illustrated in Figure 4C.

Functional analysis of differentially expressed mRNAs in DC specimens

Besides m6A modification levels, the m6A microarray analyses provided data for mRNA expression (Figure 5A and B). A total of 12015 mRNAs in the DC and NC groups showed significantly different expression [$P \leq 0.05$, fold change (FC) ≥ 1.5], 7698 of which were upregulated, whereas 4317 were downregulated. The functions of the top 20 differentially expressed mRNAs (DEmRNAs) (Supplementary Table 2) were analyzed using GO and KEGG pathway analyses. Among the enriched GO terms, 780 BPs, 137 CCs, and 101 MFs were associated with downregulated mRNA expression, with the top 10 displayed in Figure 5C. Moreover, 1199 BPs, 119 CCs, and 190 MFs were identified to be linked to upregulated mRNA expression, with the top 10 presented in Figure 5D. Among the upregulated mRNAs of the BP category, "cellular component organization" had the highest GO term enrichment score, whereas for the downregulated mRNAs, the highest score belonged to "positive regulation of immune effector process". For the CC category, "intracellular" and "plasma membrane" were the most prominent GO terms for up- and down-regulated mRNA expression, respectively. In the MF category, "protein binding" was the most significant term for both up- and downregulated mRNAs.

According to KEGG pathway analysis, DEmRNAs participated in 55 pathways, most of which were primarily enriched in the "MAPK axis", "Type II DM", and "cAMP axis" (Figure 5E and F).

Combined analysis of m6A methylation and mRNA expression in DC samples

Using the thresholds FC ≥ 1.5 and $P \leq 0.05$, the combined analysis revealed significantly altered m6A methylation and mRNA expression levels in 1,320 mRNAs. Conjoint analysis of these 1320 mRNAs resulted in the formation of four mRNA groups: Group I, 958 hypermethylated and upregulated mRNAs; Group II, 105 hypermethylated and downregulated mRNAs; Group III, 207 hypomethylated and downregulated mRNAs; Group IV, 50 hypomethylated and upregulated mRNAs (Figure 6A). Several key genes of ferroptosis (*PRNP*, *SLC39A8*, *VDAC2*, *P53*, *CYBB*, *ATG7*, and *SLC3A2*) were found in Group I.

Hypermethylated-upregulated (hyper-up) and -downregulated (hypo-down) mRNAs were further identified using GO and KEGG pathway analyses. For Group I mRNAs, the most enriched GO terms in BP, CC, and MF categories were found to be "protein membrane anchor", "early phagosome", and "sodium ion binding", respectively. For Group III mRNAs, the terms were "lens fiber cell development", "cohesin complex", and "translation release factor activity binding" (Figure 6B). KEGG pathway analysis showed that DEmRNAs participated in 26 pathways. Most mRNAs in Group I were mainly enriched in "alpha-linolenic acid metabolism," "ferroptosis", and "apoptosis", whereas Group III mRNAs were primarily enriched in "calcium axis", "cGMP-PKG axis", and "tight junction" (Figure 6C and D).

Validation of the diverse methylated mRNA and RNA methyltransferase expression patterns in vivo and in vitro

We randomly selected four mRNAs (BECN2, METTL21A, NFE2, and TIPRL) for MeRIP-qPCR to validate the microarray data quality; specifically, we screened the differentially methylated mRNAs under the criteria of P value ≤ 0.05 and FC ≥ 1.5, and then we selected genes with multiple expression folds for verification with the primers can be designed for those mRNAs. Finally, we selected 4 methylated mRNAs with different fold changes for verification to ensure the reliability of the results to a certain extent. Details of the selected genes are listed in Supplementary Table 3, and the results accorded with the microarray data (Figure 7A). Furthermore, to explore the possible genes participating in m6A modification, we compared the expression of the DEmRNAs in our epitranscriptomic micro-array with that of 24 known methylation-related genes (METTL3, METTL14, WTAP, VIRMA, KIAA1429, RNA binding motif protein 15 (RBM15), RBM15B, ALKBH5, FTO, AlkB-H9, HNRNPA2, HNRNPB1, HNRNPC1, HNRNPC2, YTHDC1, YTHDC2, YTHDF1, YTHDF2, YTHDF3, EIF3A, EIF3B, IGF2BPs, DGCR8, and ELAVL1). The expression of five genes (RBM15, WTAP, ALKBH5, FTO, and YTHDF1) was found to be upregulated in the microarray results (Figure 7B; the FC values of these genes are shown in Figure 7C); and of these, RBM15 exhibited the highest change in expression level. Additionally, the upregulation of RBM15 in SRA01/04 cells cultured in HG medium verified its expression *in vitro*, supporting the qRT-PCR results in DC specimens (Figure 7D).

Table 2 The top 20 most hyper- and hypomethylated mRNAs

Gene symbol	*P* value	Fold change	Regulation	Chromosome
AQP2	0.001135123	3.60	Hyper	chr12
RPL10	0.001594064	3.40	Hyper	chrX
ACP5	0.004544885	3.25	Hyper	chr19
ACAP1	0.003944032	3.21	Hyper	chr17
CALML6	0.00484061	3.05	Hyper	chr1
DDX31	1.02006E-05	3.04	Hyper	chr9
KRTAP29-1	3.59728E-05	2.97	Hyper	chr17
TRIM39-RPP21	0.001179594	2.95	Hyper	chr6
DGCR8	0.013600714	2.90	Hyper	chr22
LRAT	0.001067196	2.90	Hyper	chr4
NR1H3	0.028959935	5.78	Hypo	chr11
PNPT1	0.001479448	4.99	Hypo	chr2
TSEN2	0.015094744	4.99	Hypo	chr3
C3orf80	0.000939962	4.61	Hypo	chr3
TBCD	0.001813039	4.61	Hypo	chr17
RPS19	0.004668423	4.12	Hypo	chr19
TEAD2	0.031922173	4.02	Hypo	chr19
RAB3IP	0.005656491	3.96	Hypo	chr12
HN1L	0.008004647	3.77	Hypo	chr16
TFEB	0.004349132	3.70	Hypo	chr6

DISCUSSION

The present study elucidated the m6A landscape in DC using an epitranscriptomic microarray, which simultaneously analyzed the methylation and expression of related mRNA. According to the microarray results, a total of 1345 mRNAs exhibiting significantly different m6A modification levels between DC cases and NCs were identified. Most of these mRNAs (1125/1345) had higher m6A methylation levels in the DC samples. First identified in the 1970s, abundant m6A modifications in polyadenylated RNA were accidentally discovered by some research groups when they were characterizing the 5′ structures of mRNA in mammalian cells[12]. In multiple human pathophysiological processes, m6A extensively modifies RNA transcription and protein generation[13]. Modification by m6A modulates gene expression by affecting mRNA splicing, localisation, stability, and translation. Over the past few years, the development of techniques such as MeRIP-sequencing and epitranscriptomic microarrays has made the high-throughput measurement of m6A modification sites possible[14-16]. These approaches allow simultaneous screening of modified transcript types and modification changes under different con-ditions, as well as detection of modification proportions per transcript. The development of microarray method has allowed for a more subtle mapping of the m6A modification, providing better insights into its importance in gene regulation.

In this study, RBM15 was found most upregulated in the DC group, which was verified in DC samples and HG-cultured LECs. Methylation through m6A is a reversible process, dynamically regulated by three different types of protein complexes: methyltransferases, demethylases, and readers[17]. RBM15 and its paralog, RBM15B, are additional components of the methyltransferase complex[18]. RBM15, a split-end protein family member, modulates m6A methylation for RNA modification[19]. As part of the methyltransferase complex, it participates in hematopoietic cell homeostasis and alternative mRNA splicing[20]. The main role of RBM15 in m6A methylation catalysis is recruiting the m6A methyltransferase complex to U-rich regions adjacent to m6A sites[18,21]. Pollreisz *et al*[22] reported markedly increased global mRNA m6A methylation level and RBM15 expression in laryngeal squa-mous cell cancer patients; however, inhibiting RBM15 led to a notable reduction in the m6A methylation level. But the potential roles played by RBM15 in DC pathogenicity need further research. It could be suggested that RBM15-mediated m6A modification of LECs may promote DC progression. Further studies are warranted to clarify the mechanisms underlying m6A modification in DC.

Further, based on the KEGG pathway analysis, ferroptosis was identified as one of the most enriched pathways in the m6A-hypermethylated and upregulated mRNAs in DC samples (Figure 4C). In human lens development, LECs play a key role in transport, metabolism, and detoxification[23]. The integrity and survival of LECs are critical for lens transparency[24]. LEC death due to apoptosis and autophagy plays pathophysiological roles in DC progression[25].

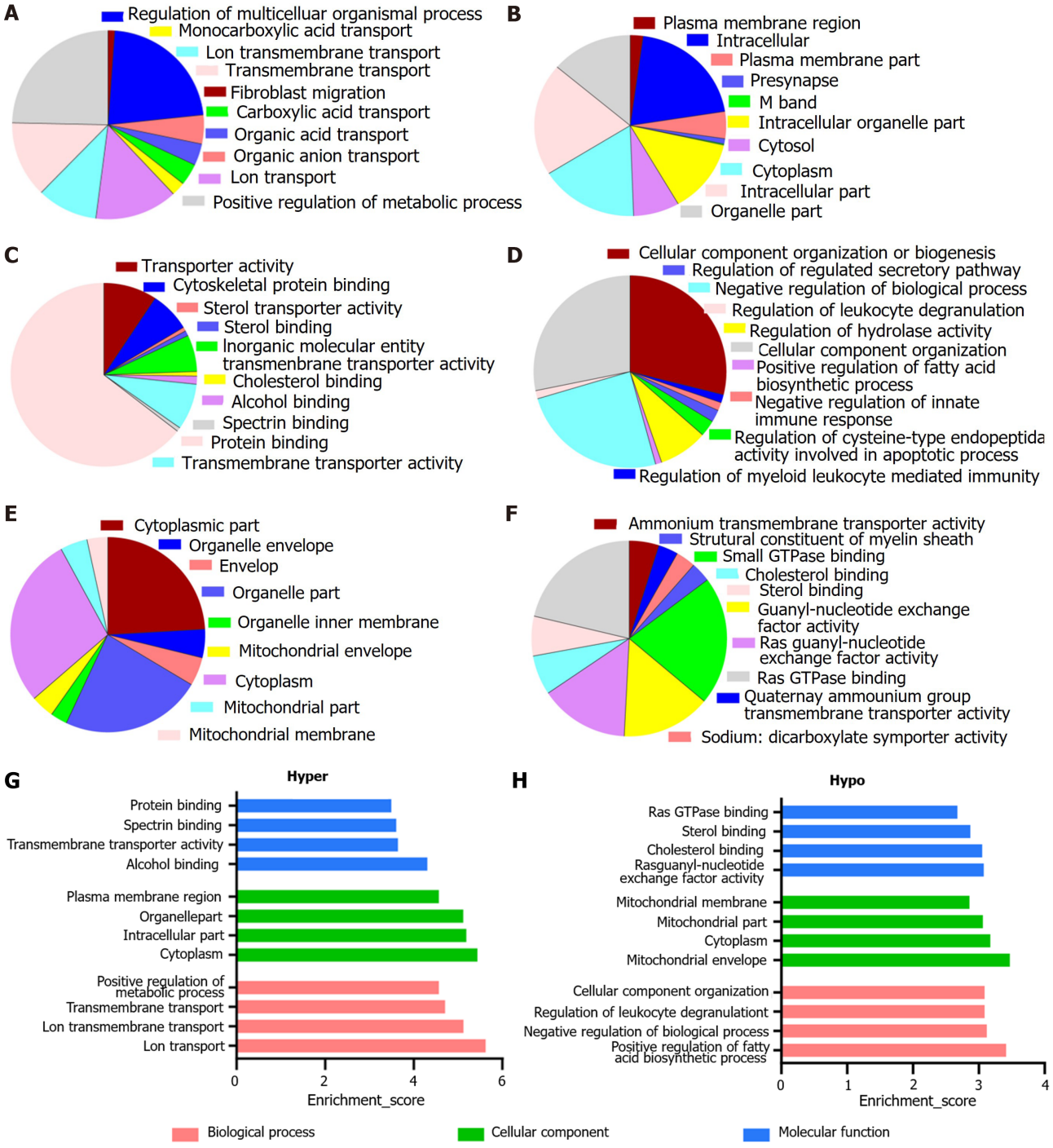

DOI: 10.4239/wjd.v14.i7.1077

Figure 3 Overall distribution of Gene Ontology analysis. A-C: Classification of hypermethylated mRNAs in the biological process (BP), cellular component (CC), and molecular function (MF) categories. Among the enriched Gene Ontology (GO) terms, 580 BPs, 110 CCs, and 100 MFs had higher mRNA methylation levels; D-F: Classification of hypomethylated mRNAs in the BP, CC, and MF categories. For the hypomethylated mRNAs, 288 BPs, 47 CCs, and 67 MFs were identified; G: The top four most enriched GO terms of the hypermethylated mRNAs; H: The top four most enriched GO terms of the hypomethylated mRNAs.

Ferroptosis is a newly defined programmed death mode that is implicated in various reactive oxygen species (ROS)-related pathophysiological states, such as age-related macular degeneration and cardiovascular diseases[26,27]. OS is vital in DC pathogenesis[28]. The process of ferroptosis is characterized by glutathione (GSH) depletion, lipid peroxidation, and intracellular ROS accumulation with iron overload as well as accelerated cell death[29-31]. GSH levels are markedly lower in DC patients than in non-diabetic senile cataract patients and non-diabetic type 2 DM patients as well as in healthy individuals[32].

The subsequent combined analysis of m6A methylation and mRNA expression levels showed several ferroptosis-associated key genes (PRNP, SLC39A8, VDAC2, P53, CYBB, ATG7, and SLC3A2) to be hypermethylated and upregulated in the DC group, suggesting enhanced ferroptosis in LECs of patients with DC. P53 can potentiate ferroptosis by inhibiting the transcription of system xc-subunit SLC7A11[33]. Reportedly, its expression was upregulated in the LECs of

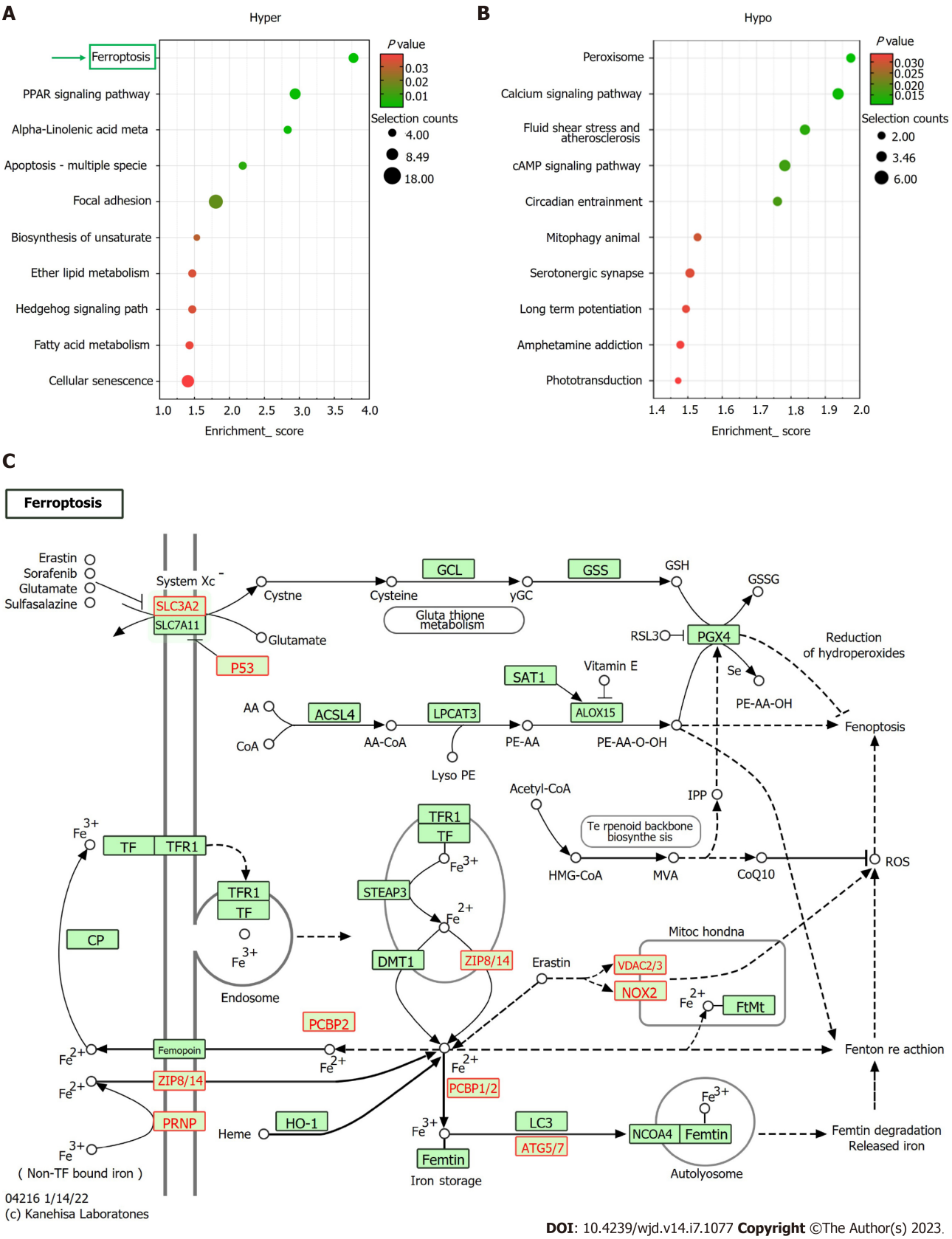

DOI: 10.4239/wjd.v14.i7.1077

Figure 4 Kyoto encyclopedia of Genes and Genomes pathway analysis. A: The top 10 Kyoto Encyclopedia of Genes and Genomes (KEGG) pathways of hypermethylated mRNAs; ferroptosis is the most enriched axis; B: The top 10 KEGG pathways of hypomethylated mRNAs; C: The KEGG map of ferroptosis pathway.

patients with DC[34]. Therefore, we speculate that m6A mRNA modifications of LECs are involved in DC progression *via* the ferroptosis pathway. In future, more comprehensive research is warranted to elucidate ferroptosis-associated mechanisms in DC pathogenesis.

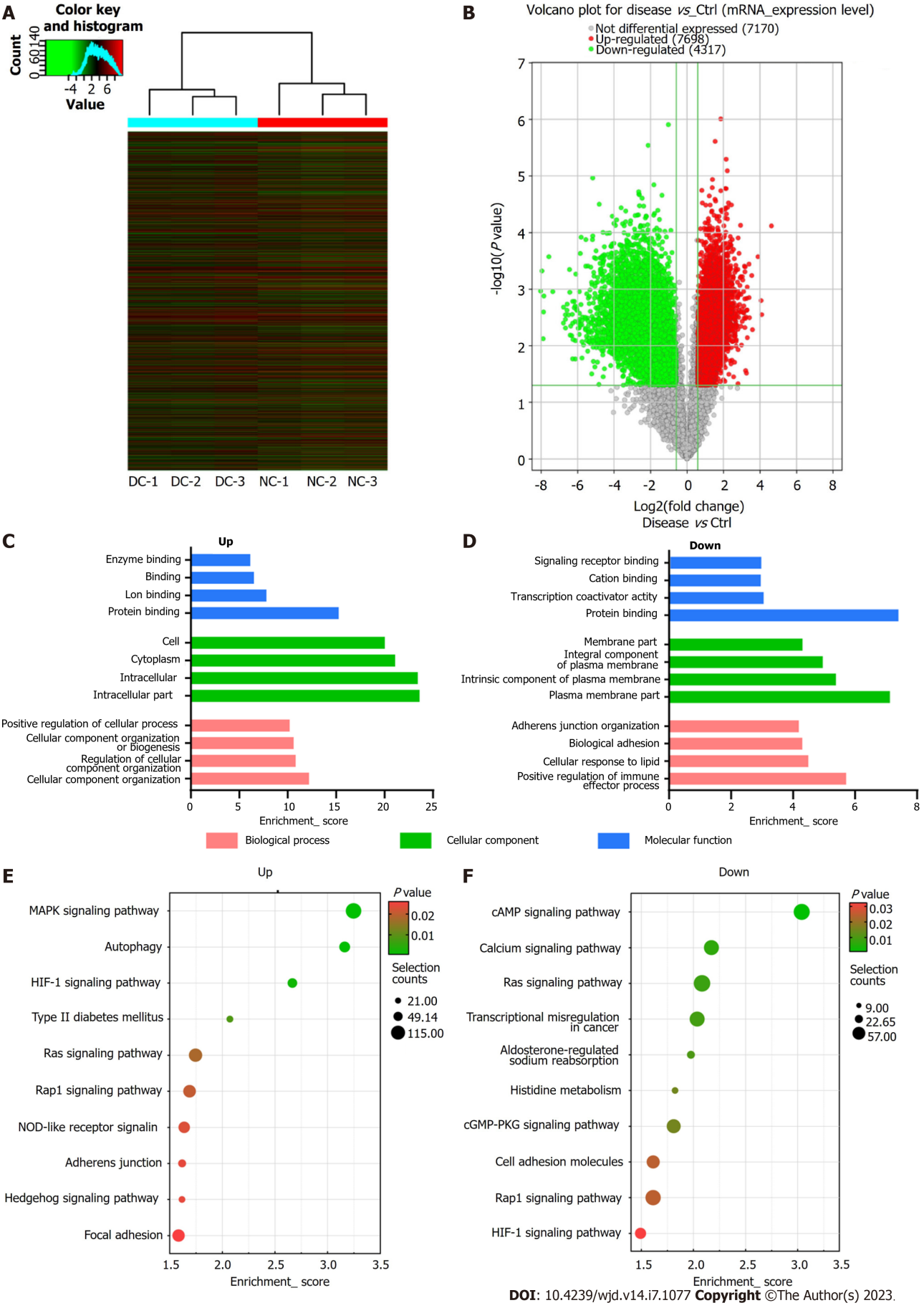

DOI: 10.4239/wjd.v14.i7.1077

Figure 5 Microarray data showing the profiles of differentially expressed mRNAs. A: Visualization of differentially expressed mRNAs (DEmRNAs)

profiles between diabetic cataract (DC) cases and normal controls (NCs) through heat map and hierarchical clustering, where red and green colors indicate up- and down-regulated mRNAs, respectively; B: Volcano plot showing significant dysregulation of 12015 mRNAs in DC cases than in NCs; C and D: The top four most enriched Gene Ontology terms of down- (C) and up-regulated mRNAs (D); E and F: The top 10 Kyoto Encyclopedia of Genes and Genomes pathways of down (E) and up-regulated mRNAs (F).

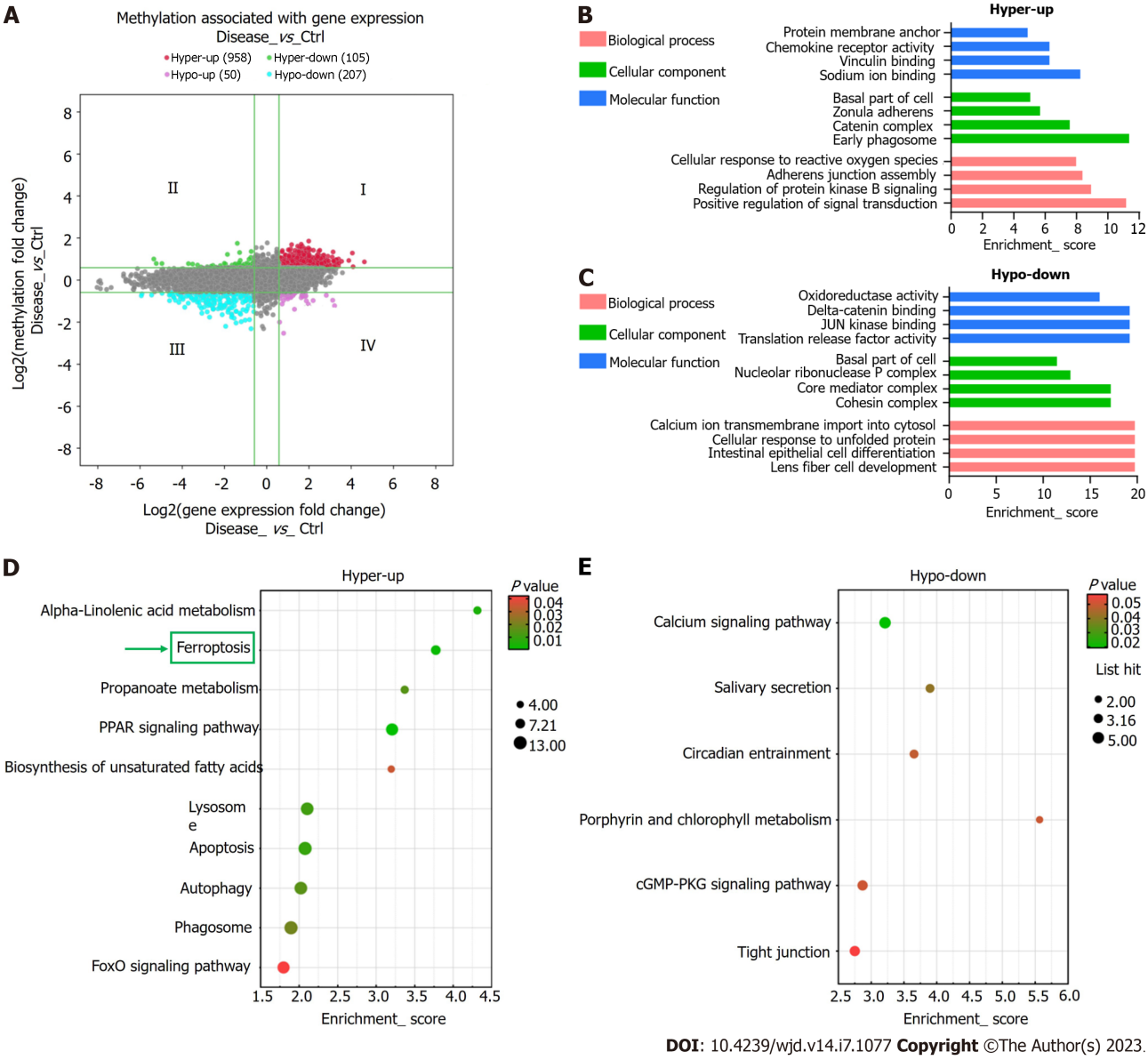

DOI: 10.4239/wjd.v14.i7.1077

Figure 6 Combined analysis of N6-methyladenosine methylation and mRNA expression levels. A: Visualization of the positive correlation of differential N6-methyladenosine methylation with differential mRNA expression *via* a four-quadrant graph; B and C: The top four Gene Ontology terms significantly enriched for the hypermethylated-upregulated (hyper-up) genes (B) and the hypomethylated-downregulated (hypo-down) genes (C); D and E: The top 10 Kyoto Encyclopedia of Genes and Genomes pathways significantly enriched for the hyper-up (D) and hypo-down genes (E).

CONCLUSION

Collectively, the m6A abundance level in total mRNA increased in patients with DC. Conjoint analysis indicated that m6A mRNA modifications of LECs might be involved in DC progression *via* the ferroptosis pathway. The expression level of RBM15 increased, which provided a better understanding of the mechanisms underlying upregulated m6A demethylation levels.

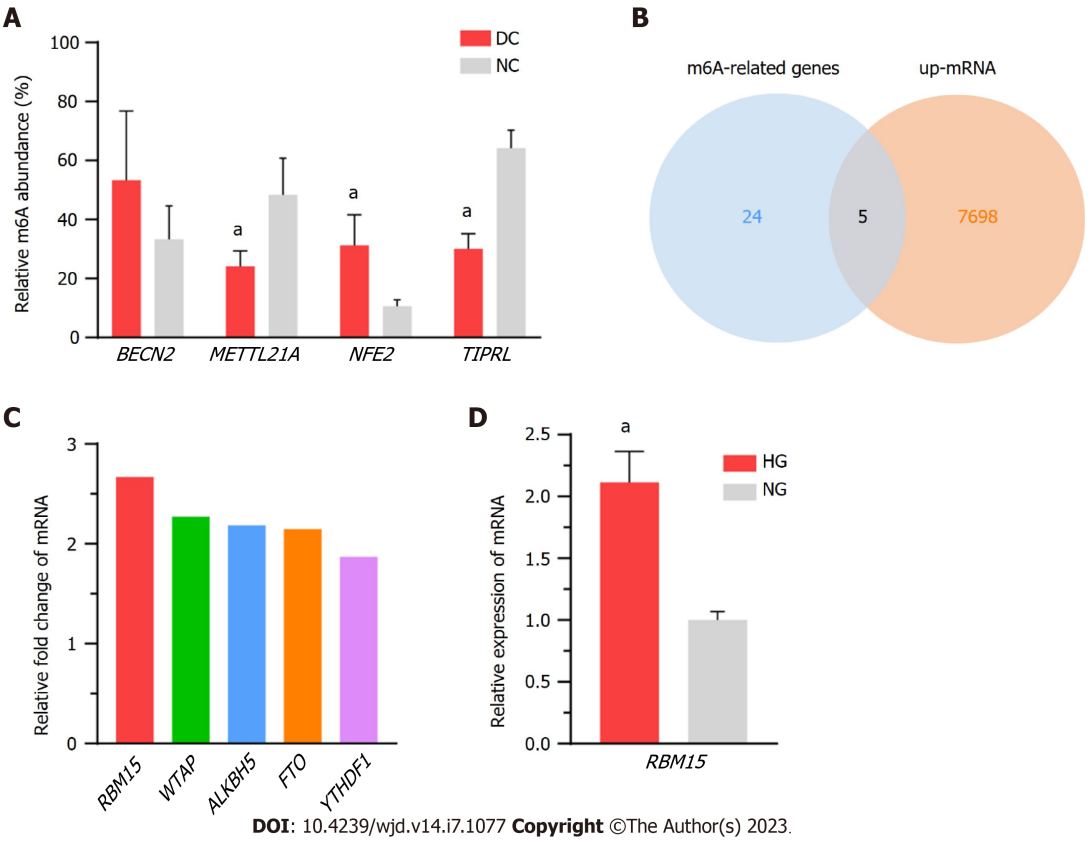

DOI: 10.4239/wjd.v14.i7.1077

Figure 7 Validation of the diverse expression levels of methylated mRNA and RNA methyltransferase, using *in vivo* and *in vitro* models. A: Methylation levels of *BECN2*, *METTL21A*, *NFE2*, and *TIPRL* are consistent with the microarray data for the diabetic cataract and normal control groups; B: Intersection results of upregulated mRNAs and N6-methyladenosine-related genes; C: Fold change values of five genes (*RBM15*, *WTAP*, *ALKBH5*, *FTO*, and *YTHDF1*) in microarray results; D: The mRNA levels of *RBM15* are significantly higher in high-glucose cultured SRA01/04 cells than in normal-glucose cultured ones. DC: Diabetic cataract; NC: Normal control; HG: High-glucose; NG: Normal-glucose. $^{a}P < 0.05$.

ARTICLE HIGHLIGHTS

Research background

Cataract remains a prime reason for visual disturbance and blindness all over the world, despite successful surgical replacement with artificial lenses. Diabetic cataract (DC) usually occurs at an earlier age with more rapid progression than age-related cataracts. The polyol pathway, oxidative stress, and nonenzymatic glycation have been shown to be linked to the pathogenesis of DC. But the exact molecular mechanisms underlying DC progression remains largely unknown. As environmental factors play critical roles in the pathogenesis of diabetes mellitus, epigenetic changes may be particularly important.

Research motivation

Despite successful surgical replacement with artificial lenses, cataract remains a prime reason for visual disturbance and blindness globally. It has been recently suggested that N6-methyladenosine (m6A) plays a role in DC progression. However, there exists a lack of understanding regarding RNA m6A modifications and the role of m6A in DC pathogenesis.

Research objectives

To investigate the roles played by altered m6A and differentially expressed mRNAs (DEmRNAs) in DC.

Research methods

M6A epitranscriptomic microarray was used to investigate altered m6A modifications and determine DEmRNAs. The possible roles played by dysregulated m6A modification was predicted through Gene Ontology and Kyoto Encyclopedia of Genes and Genomes pathway enrichment analyses. Real-time polymerase chain reaction was carried out to identify dysregulated expression patterns of RNA methyltransferases, demethylases, and readers.

Research results

Increased m6A abundance levels were found in the total mRNA of DC samples. Bioinformatics analysis predicted that ferroptosis pathways could be associated with m6A-modified mRNAs. The levels of five methylation-related genes-

RBM15, WTAP, ALKBH5, FTO, and YTHDF1-were upregulated in DC samples. Upregulation of RBM15 expression was verified in SRA01/04 cells with high-glucose medium and in samples from patients with DC.

Research conclusions

M6A abundance level in total mRNA increased in patients with DC. Ferroptosis pathways could be associated with m6A-modified mRNAs.

Research perspectives

M6A mRNA modifications may be involved in DC progression *via* the ferroptosis pathway.

FOOTNOTES

Author contributions: Cai L and Han XY contributed equally to this work; Lu Y and Yang J contributed equally to this work; Cai L performed the experiments, analyzed the data, and wrote the original draft; Han XY collected the samples, performed the experiments, and also wrote the original draft; Li D designed the experiments; Ma DM and Shi YM performed the experiments; Lu Y and Yang J designed the experiments and revised the draft; and all authors read and approved the final manuscript.

Supported by the National Natural Science Foundation of China, No. 82171039.

Institutional review board statement: This study was reviewed and approved by the Ethics Committee of the Eye and ENT Hospital of Fudan University (approval No. 2013021).

Informed consent statement: Written informed consent was obtained from all patients.

Conflict-of-interest statement: The authors declare that the research was conducted in the absence of any commercial or financial relationships that could be construed as a potential conflict of interest.

Data sharing statement: The data for this study can be obtained from the corresponding author upon request.

ARRIVE guidelines statement: The authors have read the ARRIVE guidelines, and the manuscript was prepared and revised according to the ARRIVE guidelines.

Country/Territory of origin: China

ORCID number: Lei Cai 0000-0001-6241-6261; Xiao-Yan Han 0000-0001-7016-8659; Dan Li 0000-0002-8841-8991; Dong-Mei Ma 0000-0001-5031-7549; Yu-Meng Shi 0000-0001-9612-8989; Yi Lu 0000-0002-0245-7392; Jin Yang 0000-0002-3556-0046.

S-Editor: Chen YL
L-Editor: A
P-Editor: Chen YX

REFERENCES

1 **Andley UP**. The lens epithelium: focus on the expression and function of the alpha-crystallin chaperones. *Int J Biochem Cell Biol* 2008; **40**: 317-323 [PMID: 18093866 DOI: 10.1016/j.biocel.2007.10.034]
2 **Bertrand RL**. Iron accumulation, glutathione depletion, and lipid peroxidation must occur simultaneously during ferroptosis and are mutually amplifying events. *Med Hypotheses* 2017; **101**: 69-74 [PMID: 28351498 DOI: 10.1016/j.mehy.2017.02.017]
3 **Cao JY**, Dixon SJ. Mechanisms of ferroptosis. *Cell Mol Life Sci* 2016; **73**: 2195-2209 [PMID: 27048822 DOI: 10.1007/s00018-016-2194-1]
4 **Chen L**, Chen Y, Ding W, Zhan T, Zhu J, Zhang L, Wang H, Shen B, Wang Y. Oxidative Stress-Induced TRPV2 Expression Increase Is Involved in Diabetic Cataracts and Apoptosis of Lens Epithelial Cells in a High-Glucose Environment. *Cells* 2022; **11** [PMID: 35406761 DOI: 10.3390/cells11071196]
5 **Chokkalla AK**, Mehta SL, Kim T, Chelluboina B, Kim J, Vemuganti R. Transient Focal Ischemia Significantly Alters the m(6)A Epitranscriptomic Tagging of RNAs in the Brain. *Stroke* 2019; **50**: 2912-2921 [PMID: 31436138 DOI: 10.1161/STROKEAHA.119.026433]
6 **Chylack LT Jr**, Wolfe JK, Singer DM, Leske MC, Bullimore MA, Bailey IL, Friend J, McCarthy D, Wu SY. The Lens Opacities Classification System III. The Longitudinal Study of Cataract Study Group. *Arch Ophthalmol* 1993; **111**: 831-836 [PMID: 8512486 DOI: 10.1001/archopht.1993.01090060119035]
7 **Desrosiers R**, Friderici K, Rottman F. Identification of methylated nucleosides in messenger RNA from Novikoff hepatoma cells. *Proc Natl Acad Sci U S A* 1974; **71**: 3971-3975 [PMID: 4372599 DOI: 10.1073/pnas.71.10.3971]
8 **Dixon SJ**, Lemberg KM, Lamprecht MR, Skouta R, Zaitsev EM, Gleason CE, Patel DN, Bauer AJ, Cantley AM, Yang WS, Morrison B 3rd,

Stockwell BR. Ferroptosis: an iron-dependent form of nonapoptotic cell death. *Cell* 2012; **149**: 1060-1072 [PMID: 22632970 DOI: 10.1016/j.cell.2012.03.042]

9 **Dominissini D**, Moshitch-Moshkovitz S, Salmon-Divon M, Amariglio N, Rechavi G. Transcriptome-wide mapping of N(6)-methyladenosine by m(6)A-seq based on immunocapturing and massively parallel sequencing. *Nat Protoc* 2013; **8**: 176-189 [PMID: 23288318 DOI: 10.1038/nprot.2012.148]

10 **Fu Y**, Dominissini D, Rechavi G, He C. Gene expression regulation mediated through reversible m^{6}A RNA methylation. *Nat Rev Genet* 2014; **15**: 293-306 [PMID: 24662220 DOI: 10.1038/nrg3724]

11 **Hiriart E**, Gruffat H, Buisson M, Mikaelian I, Keppler S, Meresse P, Mercher T, Bernard OA, Sergeant A, Manet E. Interaction of the Epstein-Barr virus mRNA export factor EB2 with human Spen proteins SHARP, OTT1, and a novel member of the family, OTT3, links Spen proteins with splicing regulation and mRNA export. *J Biol Chem* 2005; **280**: 36935-36945 [PMID: 16129689 DOI: 10.1074/jbc.M501725200]

12 **Jain AK**, Lim G, Langford M, Jain SK. Effect of high-glucose levels on protein oxidation in cultured lens cells, and in crystalline and albumin solution and its inhibition by vitamin B6 and N-acetylcysteine: its possible relevance to cataract formation in diabetes. *Free Radic Biol Med* 2002; **33**: 1615-1621 [PMID: 12488130 DOI: 10.1016/s0891-5849(02)01109-7]

13 **Jiang L**, Kon N, Li T, Wang SJ, Su T, Hibshoosh H, Baer R, Gu W. Ferroptosis as a p53-mediated activity during tumour suppression. *Nature* 2015; **520**: 57-62 [PMID: 25799988 DOI: 10.1038/nature14344]

14 **Kaliaperumal R**, Venkatachalam R, Nagarajan P, Sabapathy SK. Association of Serum Magnesium with Oxidative Stress in the Pathogenesis of Diabetic Cataract. *Biol Trace Elem Res* 2021; **199**: 2869-2873 [PMID: 33037494 DOI: 10.1007/s12011-020-02429-9]

15 **Klungland A**, Dahl JA. Dynamic RNA modifications in disease. *Curr Opin Genet Dev* 2014; **26**: 47-52 [PMID: 25005745 DOI: 10.1016/j.gde.2014.05.006]

16 **Lim SA**, Joo CK, Kim MS, Chung SK. Expression of p53 and caspase-8 in lens epithelial cells of diabetic cataract. *J Cataract Refract Surg* 2014; **40**: 1102-1108 [PMID: 24957431 DOI: 10.1016/j.jcrs.2013.12.015]

17 **McCarty CA**, Taylor HR. Recent developments in vision research: light damage in cataract. *Invest Ophthalmol Vis Sci* 1996; **37**: 1720-1723 [PMID: 8759338]

18 **Meyer KD**, Jaffrey SR. Rethinking m(6)A Readers, Writers, and Erasers. *Annu Rev Cell Dev Biol* 2017; **33**: 319-342 [PMID: 28759256 DOI: 10.1146/annurev-cellbio-100616-060758]

19 **Ogurtsova K**, da Rocha Fernandes JD, Huang Y, Linnenkamp U, Guariguata L, Cho NH, Cavan D, Shaw JE, Makaroff LE. IDF Diabetes Atlas: Global estimates for the prevalence of diabetes for 2015 and 2040. *Diabetes Res Clin Pract* 2017; **128**: 40-50 [PMID: 28437734 DOI: 10.1016/j.diabres.2017.03.024]

20 **Pascolini D**, Mariotti SP. Global estimates of visual impairment: 2010. *Br J Ophthalmol* 2012; **96**: 614-618 [PMID: 22133988 DOI: 10.1136/bjophthalmol-2011-300539]

21 **Patil DP**, Chen CK, Pickering BF, Chow A, Jackson C, Guttman M, Jaffrey SR. m(6)A RNA methylation promotes XIST-mediated transcriptional repression. *Nature* 2016; **537**: 369-373 [PMID: 27602518 DOI: 10.1038/nature19342]

22 **Pollreisz A**, Schmidt-Erfurth U. Diabetic cataract-pathogenesis, epidemiology and treatment. *J Ophthalmol* 2010; **2010**: 608751 [PMID: 20634936 DOI: 10.1155/2010/608751]

23 **Qin Y**, Liu Q, Tian S, Xie W, Cui J, Wang RF. TRIM9 short isoform preferentially promotes DNA and RNA virus-induced production of type I interferon by recruiting GSK3β to TBK1. *Cell Res* 2016; **26**: 613-628 [PMID: 26915459 DOI: 10.1038/cr.2016.27]

24 **Robman L**, Taylor H. External factors in the development of cataract. *Eye (Lond)* 2005; **19**: 1074-1082 [PMID: 16304587 DOI: 10.1038/sj.eye.6701964]

25 **Ru W**, Zhang X, Yue B, Qi A, Shen X, Huang Y, Lan X, Lei C, Chen H. Insight into m(6)A methylation from occurrence to functions. *Open Biol* 2020; **10**: 200091 [PMID: 32898471 DOI: 10.1098/rsob.200091]

26 **Sharma KK**, Santhoshkumar P. Lens aging: effects of crystallins. *Biochim Biophys Acta* 2009; **1790**: 1095-1108 [PMID: 19463898 DOI: 10.1016/j.bbagen.2009.05.008]

27 **Totsuka K**, Ueta T, Uchida T, Roggia MF, Nakagawa S, Vavvas DG, Honjo M, Aihara M. Oxidative stress induces ferroptotic cell death in retinal pigment epithelial cells. *Exp Eye Res* 2019; **181**: 316-324 [PMID: 30171859 DOI: 10.1016/j.exer.2018.08.019]

28 **Wang X**, Tian L, Li Y, Wang J, Yan B, Yang L, Li Q, Zhao R, Liu M, Wang P, Sun Y. RBM15 facilitates laryngeal squamous cell carcinoma progression by regulating TMBIM6 stability through IGF2BP3 dependent. *J Exp Clin Cancer Res* 2021; **40**: 80 [PMID: 33637103 DOI: 10.1186/s13046-021-01871-4]

29 **Yan G**, Yuan Y, He M, Gong R, Lei H, Zhou H, Wang W, Du W, Ma T, Liu S, Xu Z, Gao M, Yu M, Bian Y, Pang P, Li X, Yu S, Yang F, Cai B, Yang L. m(6)A Methylation of Precursor-miR-320/RUNX2 Controls Osteogenic Potential of Bone Marrow-Derived Mesenchymal Stem Cells. *Mol Ther Nucleic Acids* 2020; **19**: 421-436 [PMID: 31896070 DOI: 10.1016/j.omtn.2019.12.001]

30 **Yang J**, Liu J, Zhao S, Tian F. N(6)-Methyladenosine METTL3 Modulates the Proliferation and Apoptosis of Lens Epithelial Cells in Diabetic Cataract. *Mol Ther Nucleic Acids* 2020; **20**: 111-116 [PMID: 32163892 DOI: 10.1016/j.omtn.2020.02.002]

31 **Yu Y**, Yan Y, Niu F, Wang Y, Chen X, Su G, Liu Y, Zhao X, Qian L, Liu P, Xiong Y. Ferroptosis: a cell death connecting oxidative stress, inflammation and cardiovascular diseases. *Cell Death Discov* 2021; **7**: 193 [PMID: 34312370 DOI: 10.1038/s41420-021-00579-w]

32 **Zhang C**, Fu J, Zhou Y. A Review in Research Progress Concerning m6A Methylation and Immunoregulation. *Front Immunol* 2019; **10**: 922 [PMID: 31080453 DOI: 10.3389/fimmu.2019.00922]

33 **Zhang L**, Tran NT, Su H, Wang R, Lu Y, Tang H, Aoyagi S, Guo A, Khodadadi-Jamayran A, Zhou D, Qian K, Hricik T, Côté J, Han X, Zhou W, Laha S, Abdel-Wahab O, Levine RL, Raffel G, Liu Y, Chen D, Li H, Townes T, Wang H, Deng H, Zheng YG, Leslie C, Luo M, Zhao X. Cross-talk between PRMT1-mediated methylation and ubiquitylation on RBM15 controls RNA splicing. *Elife* 2015; **4** [PMID: 26575292 DOI: 10.7554/eLife.07938]

34 **Zhu S**, Wang JZ, Chen D, He YT, Meng N, Chen M, Lu RX, Chen XH, Zhang XL, Yan GR. An oncopeptide regulates m(6)A recognition by the m(6)A reader IGF2BP1 and tumorigenesis. *Nat Commun* 2020; **11**: 1685 [PMID: 32245947 DOI: 10.1038/s41467-020-15403-9]

Published by **Baishideng Publishing Group Inc**
7041 Koll Center Parkway, Suite 160, Pleasanton, CA 94566, USA
Telephone: +1-925-3991568
E-mail: bpgoffice@wjgnet.com
Help Desk: https://www.f6publishing.com/helpdesk
https://www.wjgnet.com